Discover Mechanical Engineering

RESEARCH Open Access

# Evaluation of mechanical reinforcement in epoxy adhesives using a hybrid triple nanoparticle reinforcement strategy based on MWCNTs, GNPs and nano alumina

Pedram Zamani[1*], Esmaeil Ghasemi Solokloo[2], Ozkan Ozbek[3], Mehmet Veysel Cakir[4], Mahmoud Shariati[5*] and Ali Hosseinzadeh[5]

*Correspondence:
Pedram Zamani
p.zamani@du.ac.ir
Mahmoud Shariati
mshariati44@um.ac.ir
[1]School of Engineering, Damghan University, Damghan, Iran
[2]Department of Mechanical Engineering, Faculty of Engineering, University of Birjand, Birjand, Iran
[3]Department of Mechanical Engineering, Faculty of Engineering, Pamukkale University, Denizli, Turkey
[4]Department of Mechanical Engineering, Faculty of Engineering and Architecture, Kilis 7 Aralik University, Kilis, Turkey
[5]Department of Mechanical Engineering, Faculty of Engineering, Ferdowsi University of Mashhad, Mashhad, Iran

## Abstract

The reinforcement of adhesives with nanoparticles has emerged as a promising strategy for enhancing their mechanical performance. Although numerous studies have explored single- and double-nanoparticle reinforcement systems, the simultaneous incorporation of three distinct nanoparticles within a single adhesive matrix—referred to here as triple-particle reinforcement—remains largely unexplored. In this context, the present research aims to take an initial step in evaluating the influence of triple-particle reinforcement with three types of nanoparticles including multi-walled carbon nanotubes (MWCNTs), graphene nanoplatelets (GNPs), and nano-alumina on tensile strength of Axson-Sika Adekit A 140-1 epoxy adhesive. Four groups of specimens were prepared to evaluate tensile strength of the bulk adhesive including neat adhesive, adhesives with single-type reinforcement using either MWCNTs, GNPs, or nano-alumina (at 0.1, 0.3, 0.5, and 0.7 wt%), adhesives with double-type reinforcement combining two nanoparticles in equal proportions, and adhesives with triple-particle reinforcement involving all three nanoparticles at equal mixing ratios across the same weight contents. The results showed that, in the double-type category, the MWCNT-GNP combination at 0.5 wt% led to the best performance, surpassing the best single-type result by 17%. It was found that the triple-particle reinforcement using a dispersion method as in the single- and double-type reinforced specimens resulted in approximately similar tensile strength compared to that of the double-type nanoparticle reinforcement. However, by modifying the dispersion method, the tensile strength was approximately equal to that of the double-particle nanoparticle reinforcement group.

**Keywords** Nanoparticle reinforcement, Adhesive, Hybrid-type reinforcement, Tensile strength, Multi-walled carbon nanotube (MWCNT), Graphene nanoplatelet (GNP)

## 1 Introduction

In the past decade, adhesively bonded joints have been extensively employed in advanced engineering applications such as aircraft structures, automotive components, wind turbine blades, aerospace systems, and marine constructions [1–5]. This widespread adoption stems from their superior characteristics compared to conventional joining techniques (e.g., welding, bolting, or riveting), including the capability to join dissimilar materials, the elimination of perforation-induced damage in composite substrates typical of bolted joints, and the ability to achieve a more uniform stress distribution across the bonded region [6, 7]. In designing bonded joints for advanced engineering structures, several design philosophies must be considered, namely, design under static loading, fatigue design, fracture mechanics-based design, and damage tolerance considerations [7, 8]. Each of these design approaches is affected by the mechanical behavior of the adhesive and substrates as well as adhesive-substrate interface (e.g., strength, life, fracture toughness). Therefore, enhancing both the intrinsic mechanical properties of the adhesive and the interfacial performance is crucial to improving the overall strength, reliability and durability of adhesively bonded joints [7, 9].

Besides several approaches proposed to enhance the strength and durability of adhesive joints-such as surface treatments and geometrical modifications (e.g., fillet geometry, overlap length, overlap surface patterning, and etc [7, 10–13])-significant attention has also been devoted to improving the intrinsic mechanical properties of the adhesive material itself and the adhesive-substrate interface through nanoparticle reinforcing techniques [9, 14–21]. In this way, several research studies have been conducted on evaluating mechanical behavior (e.g., strength, fatigue life, and energy release rate) of the adhesive material and bonded joint by inserting various nanoparticles such as multi-walled carbon nanotube (MWCNT), graphene nanoplatelet (GNP), fullerene, titanium oxide ($TiO_2$), $Al_2O_3$, $SiO_2$, boron nitride (BN), $Fe_3O_4$, and nano clay [15, 22–37]. This approach in which the mechanical properties of a specified adhesive/joint are improved by addition of a nanoparticle is known as a single-type nanoparticle reinforcement.

In recent years, only a limited number of studies have investigated the effect of incorporating two types of nanoparticles into the adhesive-known as hybrid nanoparticle reinforcement-on the mechanical performance of bonded joints [36, 38–50]. In an experimental study, Razavi et al. [38] examined the effect of inserting a mixture of MWCNTs and silica nanoparticles on the lap shear strength of adhesive-bonded joints, using aluminum substrates and UHU plus Endfest 300 epoxy adhesive. They reported that, at 0.8 wt%, the incorporation of a mixture of MWCNT and silica nanoparticles resulted in the maximum improvement in the lap shear strength compared to joints reinforced with a single type of nanoparticle (either MWCNTs or silica) at the same weight content. Zamani et al. [36] concluded that, at a given weight content, the simultaneous insertion of GNPs and silica nanoparticles in a 1:1 ratio into Araldite 2015 adhesive led to higher strength and longer fatigue life compared to reinforcement with each type of nanoparticle alone at the same weight content. In another study, Zamani et al. [40] highlighted the significant effect of the mixing ratio on the performance of hybrid nanoparticle-reinforced adhesives by GNP and silica nanoparticles. They deduced that, at 0.5 wt% and 1.0 wt%, hybrid reinforcement consisting of 70% GNPs and 30% nano-silica led to the highest four-point bending strength compared to other mixing ratios of 30:70 and 50:50 (GNP: nano-silica). However, their results indicated that, at a higher

weight content of 1.5 wt%, the 30:70 GNP: nano-silica hybrid mixing ratio resulted in the maximum strength. By examining the hybridization effect of MWCNT and nano-silica on the flexural and lap shear strengths of adhesive-bonded joints with GFRP substrates, Ozbek and Cakir [49] observed that the combination of 0.5 wt% MWCNTs and 0.25 wt% silica nanoparticles led to the greatest improvements in both flexural and lap shear strengths. Radshad et al. [42] investigated the effect of hybrid reinforcement with GNP and MWCNT nanoparticles, using MWCNT: GNP mixing ratios of 1:0, 1:1, 1:3, and 3:1, on the mode-I fracture toughness of GFRP bonded joints. They reported that, for a total additive content of 0.3 wt%, a mixture consisting of one-third GNPs and two-thirds MWCNTs resulted in a 90% increase in the adhesive's fracture energy compared with that reinforced solely with MWCNTs at the same weight content.

Based on the above review of the literature on nanoparticle reinforcement of adhesive joints, it is evident that a large body of work has explored the effect of individual nanoparticles on various mechanical responses of adhesives. Narrowing the scope to the simultaneous use of two or more nanoparticles reveals that, although there are a limited number of noteworthy studies, important questions remain unanswered. Chief among these is how far the simultaneous addition of multiple nanoparticle types can be extended, does increasing the number and variety of nanoparticles (and their respective weight fractions) always lead to continuous improvement, or is there an optimal combination of particle types, addition parameters, and concentrations. These open issues constitute a clear research gap needed to guide rational, targeted enhancement of adhesive mechanical properties via multi-nanoparticle or hybrid-nanoparticle reinforcement. The novelty of the present work therefore lies in examining the synergistic effects of binary and ternary nanoparticle mixtures on the tensile performance of a specified epoxy adhesive. The clear problem statement and the path of study are mentioned in the next section.

## 2 Problem statement and research scenario

As mentioned above, the hybrid incorporation of two types of nanoparticles into the adhesive can significantly enhance the static strength and durability of a bonded joint compared with those reinforced by each nanoparticle individually [36, 39]. Moreover, an important finding is that, regardless of the mixing ratio, hybrid reinforcement at a specified weight content can result in higher mechanical strength and durability than single-particle reinforcement even at higher weight contents [40]. This improvement can be attributed to the synergistic effects of microstructural toughening mechanisms. Furthermore, research has shown that, in the case of single-particle reinforcement of an adhesive, the strength and durability of the reinforced joint can be highly dependent on the particle dispersion method [39]. In this context, when a combination of different particles is used, applying the same dispersion procedure as for single-particle reinforcement may not be sufficient to for achieve enhanced improvements in mechanical properties. Thus, the challenges in the field of hybrid nanoparticle reinforcement of adhesives can summarized as follows: first, the feasibility of reinforcing an adhesive with more than one type of nanoparticle, and second, the adequacy of the dispersion procedure originally developed for single-particle reinforcement. Given the research studies on hybrid nanoparticle reinforcement of adhesives and the near absence of research on hybrid reinforcement involving more than two types of nanoparticles, the present study aims to

initiate a roadmap to address this knowledge gap by investigating the effect of incorporating a mixture of MWCNTs, GNPs and nano-alumina particles on the tensile properties of an epoxy adhesive. The rationale for selecting these nanoparticles was based on the hypothesis that variations in their morphology and characteristic length scale could activate different microstructural mechanisms during various stages of damage evolution within the adhesive, thereby contributing to a synergistic enhancement in performance. To this end, different groups-including neat (unreinforced), single-nanoparticle reinforced, and hybrid-reinforced adhesives-were prepared to evaluate the tensile behavior of bulk adhesive specimens. Subsequently, as the main focus of the study, the effect of triple nanoparticle incorporation (MWCNT-GNP-nano-alumina) and the efficiency of the dispersion procedure on the tensile performance of the epoxy adhesive was investigated. Four specimen groups were prepared including neat adhesive, adhesive reinforced with single nanoparticle types, adhesive reinforced with binary nanoparticle combinations, and adhesive reinforced with a ternary mixture. For each nanoparticle-containing group, weight fractions of 0.1, 0.3, 0.5, and 0.7 wt% were fabricated. Finally, mechanical tensile testing together with scanning electron microscopy (SEM) inspections were then employed to identify the practical limits of simultaneous nanoparticle addition and to elucidate the governing failure and toughening mechanisms.

## 3 Experimental procedure

### 3.1 Materials and specimens

A two-component epoxy adhesive, Axson-Sika Adekit A 140-1 (Sika AG Co.), a multipurpose adhesive suitable for composite and metallic structures in automotive, aeronautical, and other advanced composite applications, was employed to prepare the bulk tensile specimens. MWCNT, GNP, and nano-alumina particles (VCN materials, Boushehr, Iran) were selected as representatives of tubular, planar, and semi-spherical shaped morphologies, respectively, to reinforce the adhesive. The specifications of these nanoparticles are presented in Table 1.

Bulk specimens for tensile testing were prepared in accordance with ASTM D638 (Fig. 1). Four main tensile bulk specimen groups were fabricated: (I) Neat adhesive (no particles), (II) single-particle reinforcement at weight contents of 0.1, 0.3, 0.5, 0.7 wt%, (III) Binary-particle reinforcement with a 1:1 mixing ratio at weight contents of 0.1, 0.3, 0.5, and 0.7 wt%, (IV) Ternary-particle reinforcement with a 1:1:1 mixing ratio at weight contents of 0.1, 0.3, 0.5, and 0.7 wt%. After preparing the resin and hardener for each specimen group, silicon molds, designed according to the geometric dimensions specified in ASTM D638, were employed to fabricate the tensile bulk specimens. Following the adhesive manufacturer's instruction, bulk specimens were initially cured at room temperature for 24 h, followed by a post-curing step at 70 °C for 16 h. Group I served as the reference specimen group for comparison purposes, whereas group II was

**Table 1** Features of MWCNT, GNP, and nano-alumina particles

| | GNP | MWCNT | Alumina-gamma |
|---|---|---|---|
| Purity (%) | 99.5 | 95 | 99.99 |
| Diameter | 1–20 µm | 20–30 nm | 20 nm |
| Thickness (nm) | ≤ 40 nm | – | – |
| Length (micro meter) | – | 5–10 µm | – |
| Density (g/cm$^3$) | 1.9–2.2 | – | 3.5–3.9 |
| Specific surface (m$^2$/g) | ≥ 150 | 100 | 130–220 |

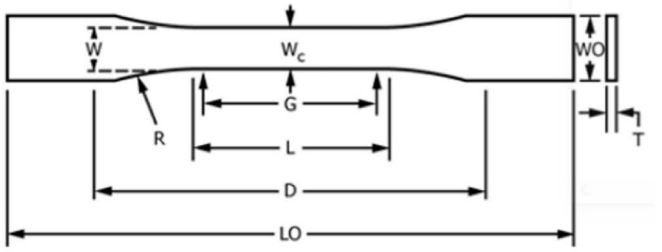


| W (mm) | 13 |
|---|---|
| L (mm) | 57 |
| LO (mm) | 165 |
| G (mm) | 50 |
| R (mm) | 76 |
| D (mm) | 115 |
| WO (mm) | 19 |
| T (mm) | 3.2 |

**Fig. 1** Geometrical dimensions of the tensile bulk specimens


(a)

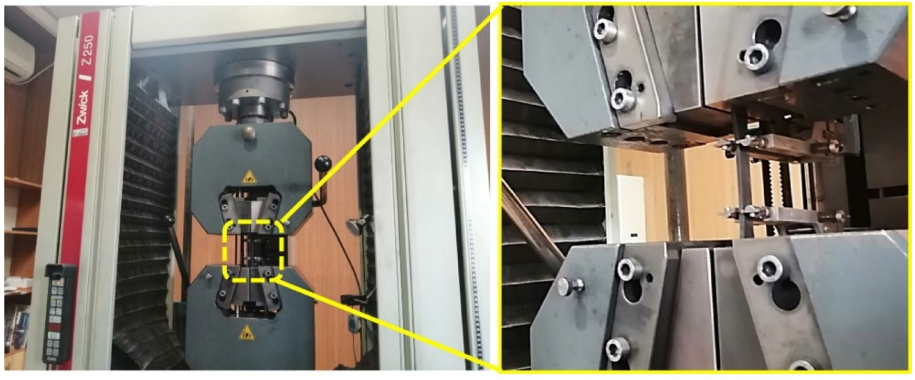


(b)

**Fig. 2** **a** Specimen fabrication, **b** tensile testing

designed to determine the optimal weight content for each type of single-nanoparticle-reinforced bulk specimen. Groups III and IV were designed to investigate the effect of hybrid reinforcement under different dispersion methods. After preparation of the bulk specimens, tensile tests were performed using a Zwick Z250 testing machine (Germany). Figure 2 illustrates the fabrication process and mechanical testing setup of the tensile bulk specimens. Table 2 presents the classification and designation of the different specimen groups. According to this table and considering four repeats for each test case, total number of 116 tensile tests were performed.

### 3.2 Nanoparticle dispersion procedure

The procedure applied for dispersing nanoparticles and its processing parameters (e.g., duration, power, and speed) within a matrix (e.g., adhesive or resin) can significantly

**Table 2** Classification of specimen groups and design of experiments

| | Additive | Weight content (wt%) | Name |
|---|---|---|---|
| *Group I* | | | |
| No reinforcement | – | 0 | Neat |
| *Group II* | | | |
| Single-type reinforcement | MWCNT | 0.1 | MWCNT-w1 |
| | | 0.3 | MWCNT-w2 |
| | | 0.5 | MWCNT-w3 |
| | | 0.7 | MWCNT-w4 |
| | GNP | 0.1 | GNP-w1 |
| | | 0.3 | GNP-w2 |
| | | 0.5 | GNP-w3 |
| | | 0.7 | GNP-w4 |
| | Alumina | 0.1 | Alumina-w1 |
| | | 0.3 | Alumina-w2 |
| | | 0.5 | Alumina-w3 |
| | | 0.7 | Alumina-w4 |
| *Group III* | | | |
| Double-particle reinforcement | MWCNT-GNP | 0.1 | M-G-w1 |
| | | 0.3 | M-G-w2 |
| | | 0.5 | M-G-w3 |
| | | 0.7 | M-G-w4 |
| | MWCNT-Alumina | 0.1 | M-A-w1 |
| | | 0.3 | M-A-w2 |
| | | 0.5 | M-A-w3 |
| | | 0.7 | M-A-w4 |
| | GNP-Alumina | 0.1 | G-A-w1 |
| | | 0.3 | G-A-w2 |
| | | 0.5 | G-A-w3 |
| | | 0.7 | G-A-w4 |
| *Group IV* | | | |
| Triple-particle reinforcement | MWCNT-GNP-Alumina | 0.1 | MGA-w1 |
| | | 0.3 | MGA-w2 |
| | | 0.5 | MGA-w3 |
| | | 0.7 | MGA-w4 |

influence the uniformity of particle distribution and minimize dispersion-induced defects such as agglomeration or particle breakage [39]. In the road map for designing nanoparticle-reinforced adhesives, sufficient attention should be paid to the dependence of the dispersion procedure on the type and morphology of the nanoparticles. In the case of a hybrid-type reinforcement, the dispersion procedure optimized for single-type reinforcement of each nanoparticle may not be suitable for achieving a uniformly reinforced material [40]. Hence, in the present research, two groups of dispersion procedures were considered: (1) dispersion procedure A which was used for group II, III, and IV of specimens, and (2) dispersion procedure B for group IV of specimens. In the dispersion procedure A, firstly, due to high viscosity of the resin, acetone was added to the resin with 1:1 mixing ratio, hand mixed for 5 min, and magnetic stirred for at 200 rpm for 10 min. Secondly, specified weight content of a particle (MWCNT, GNP, or nano alumina) was inserted to the acetone-resin solution and magnetic stirred at 200 rpm for 15 min. Thirdly, mixture of acetone, resin, and single nanoparticle were sonicated using ultrasonic bath sonication device (Elma S40H, Elmasonics, Germany) at 37 kHz frequency for 60 min. It should be noted that the temperature of the resin-acetone-GNP

mixture was controlled by immersing the beaker in an ice-water bath to prevent excessive heating. In the fourth step, the beaker was placed in a vacuum chamber to remove the air bubbles trapped within the mixture. In the final step, to exclude any remaining air bubbles trapped and to evaporate the residual acetone, the beaker was placed in a vacuum oven at 40 °C for 120 min. The evaporation of acetone content was monitored by accurately weighing the resin-acetone-nanoparticle mixture every 20 min. For hybrid-type reinforcement by two particles, simultaneous insertion of the particles in the second step of dispersion procedure A led to decrease of mechanical properties. Thus, a minor modification was applied to the dispersion procedure A. In this modification, the first particle was added, stirred at 200 rpm for 10 min, and bath sonicated at 37 kHz for 15 min. Next, the second particle was inserted and stirred at 200 rpm for 10 min. After addition of the second particle, the mixture of resin, acetone, and two particles, were dispersed similar to the third, fourth, and fifth steps in the dispersion procedure A.

As above-mentioned, dispersion procedure B corresponds to the hybrid-type reinforcement group of specimens with triple particle reinforcement. It should be noted that during the course of investigation, it was observed that applying procedure A to the triple-particle reinforcement did not lead to any improvement in the mechanical behavior compared to the other specimen groups. Therefore, a preliminary zero-phase study was carried out to examine whether modifying the sequence of particle incorporation and slightly adjusting the processing parameters could enhance the dispersion quality. The findings of this zero-phase study indicated that sequence of particle addition plays a significant role in reducing agglomeration, particularly when each particle is followed by a stirring and sonication step. In the selected version of dispersion procedure B, the first, fourth, and fifth steps were identical to those of dispersion procedure A. However, in the second step, the first particle is added to the resin and acetone dilution, magnetic stirred at 200 rpm for 10 min, and bath sonicated for 15 min. Then, the second particle was inserted, stirred at 200 rpm for 10 min, and bath sonicated for 25 min. Next, the third particle was added and magnetic stirred for 10 min with similar speed to previous steps. In the third step, the mixture of acetone, resin, and three particles were sonicated using the bath sonication device for 75 min. Figure 3 shows the general process of the dispersion for a single-type reinforcement.

## 4 Results and discussion

### 4.1 Single-particle reinforcement

Evaluation of the tensile strength for single-type reinforcements was conducted to determine the optimum weight content and the corresponding maximum improvement for each nanoparticle type. Figure 4 depicts the average tensile strength of the single-type reinforced adhesives (MWCNT-, GNP-, and alumina-reinforced) at weight contents of 0.1, 0.3, 0.5, and 0.7 wt%. It can be observed that the maximum improvement of tensile strength, compared to that of the neat adhesive, was achieved at 0.3 wt% for MWCNT- and GNP-reinforced specimens, and 0.5 wt% for alumina-reinforced specimens, corresponding to strength enhancements of 28.3%, 36.7%, and 26.7%, respectively. These improvements can be due to activation of reinforcing mechanisms related to each of the particles (e.g., pull-out, particle breakage, and plastic void growth) [27, 36, 40], and decrease of the strength after the optimum weight content can be related to agglomeration of particles acting as stress raisers [36]. Moreover, the higher tensile strength

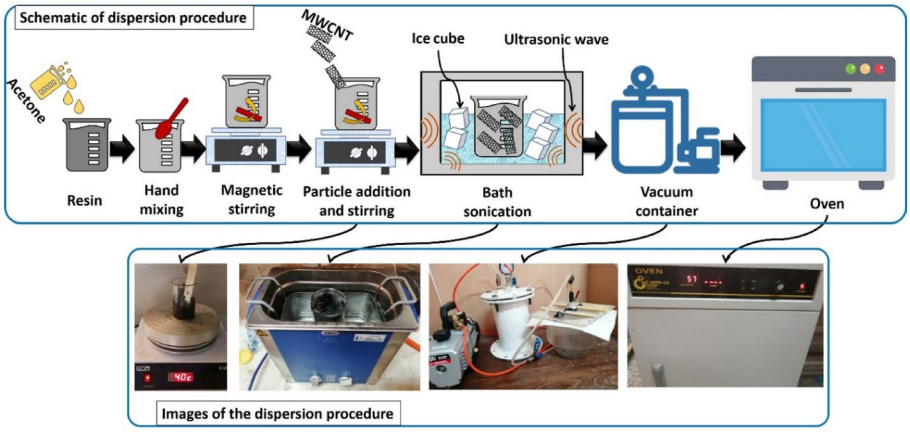


**Fig. 3** Illustration of dispersion procedure for a specified particle in the single-type reinforcement

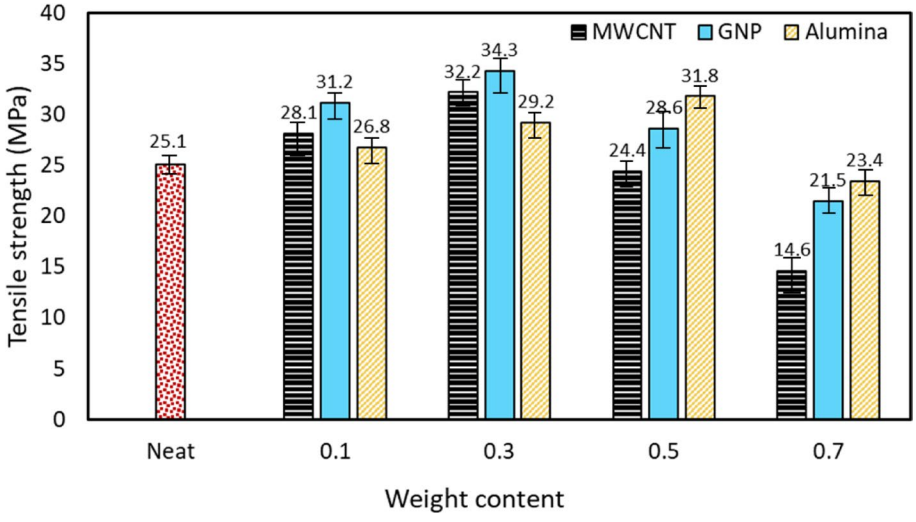


**Fig. 4** Average tensile strength of bulk adhesive specimens reinforced by single insertion of MWCNT, GNP, and alumina nanoparticles

observed in the GNP-reinforced specimens compared with those containing MWCNTs and alumina can be attributed to two main factors. First, the microscopic strengthening mechanisms in GNP-modified adhesives are more diverse. Second, their statistical distribution within a unit microscopic volume is broader. For instance, in the adhesives reinforced with GNPs, multiple mechanisms such as partial pull-out, full pull-out, particle breakage, crack path deviation, and crack arrest within the polymeric matrix were identified. In contrast, the dominant reinforcing mechanisms in the MWCNT-filled adhesives are primarily associated with pull-out, whereas in the alumina-filled samples, crack path deflection tends to be the prevailing mechanism.

### 4.2 Double-particle reinforcement

As a specified case of hybrid-type nanoparticle reinforcement, the results of the average tensile strength of double-particle reinforced adhesives by inserting mixture of MWCNT-GNP (M-G), MWCNT-Alumina (M-A), and GNP-Alumina (G-A) are presented in Fig. 5. It can be deduced that, for each weight content, mixture of MWCNT

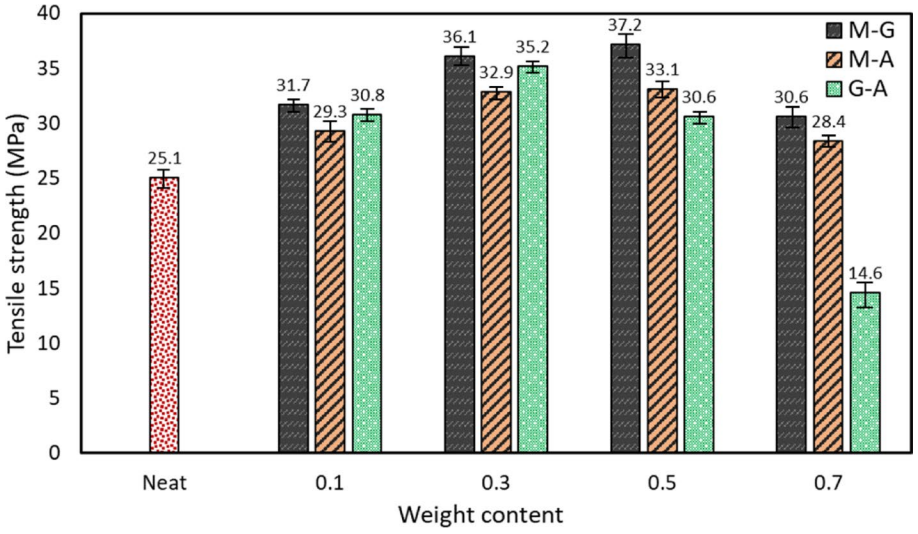


**Fig. 5** Average tensile strength of bulk adhesive specimens reinforced by double insertion of MWCNT-GNP, MWCNT-Alumina, and GNP-Alumina

**Table 3** Summary of optimum weight contents

| Reinforcement type | Best reinforcement group and wt% | Improvement description |
|---|---|---|
| Single-particle | GNP with 0.3 wt% | Improved by 36.7% compared to neat group |
| Double-particle | MWCNT-GNP with 0.5 wt% | Improved by 8.5% compared to the best case of single-particle reinforcement |
| Triple-particle | MWCNT-GNP-Alumina with 0.5 wt% | Improved by 10.5% compared to the best case of single-particle reinforcement |

and GNP with 1:1 mixing ratio led to the highest static strength compared to the MWCNT-Alumina and GNP-Alumina mixtures. For 0.1 wt%, 0.3 wt%, 0.5 wt%, and 0.7 wt% contents, double-particle reinforcement by mixing MWCNT and GNP additives led to 26.3%, 43.8%, 48.2%, and 21.9% improvements in tensile strength compared to neat specimens, respectively. It can be concluded that the optimum weight content for double-particle reinforcement with MWCNT and GNP particles is related to 0.5 wt% content, while the optimum weight content in single-type reinforcement by each of the particles is 0.3 wt% content. Also, for lower weight content of 0.1 wt%, average tensile strength of MWCNT-GNP reinforced adhesive specimens is approximately equal to the maximum value of tensile strength in single type reinforcement, which is related to GNP-reinforced specimens. However, for 0.3 wt%, 0.5 wt%, and 0.7 wt%, average tensile strength of MWCNT-GNP reinforced adhesive specimens was 5.2%, 17.0%, 30.8% greater than the maximum tensile strength obtained in the corresponding single-type reinforcements, respectively. Hence, for a specified weight content, dispersing mixture of MWCNT and GNP can lead to a higher tensile strength compared to the maximum strength obtained in the single-type reinforcement by each of the particles. Table 3 presents a clear description of optimum reinforcements for each of the single-particle and double-particle reinforcement groups. As shown in Fig. 5, the hybrid incorporation of GNP and MWCNT at each given weight fraction resulted in the highest tensile strength among all specimen groups. As previously discussed for the single-nanoparticle-reinforced specimens regarding the corresponding strengthening mechanisms, it can be

inferred here that, due to the greater diversity of microstructural reinforcement mechanisms associated with GNP-containing adhesives, combining GNP with other nanoparticles is expected to yield enhanced strength. Furthermore, the superior performance observed for the GNP–MWCNT hybrid samples may also be attributed to the significant contribution of carbon nanotubes through the pull-out mechanism.

### 4.3 Triple-particle reinforcement

As above-mentioned, hybrid-type reinforcement by inserting triple particles (MWCNT, GNP, and alumina) into the adhesive was firstly performed using the dispersion procedure A, which was applied for single-type and double-particle reinforcements. As shown in Fig. 6, for 0.1 wt%, 0.3 wt%, 0.5 wt%, and 0.7 wt%, triple-particle nanoparticle reinforcement of the adhesive by dispersion procedure A led to approximately no significant improvements compared to single-type reinforcement by each of the MWCNT, GNP, and alumina particles and lower than double-particle reinforcements. This can be related to the deficiency of dispersion procedure A in preventing the particles to agglomerate together and their adhesion to other particles. Thus, dispersion procedure B was implemented to examine dependency of triple-particle reinforcement to modification of the dispersion procedure. For 0.1 wt% content, applying triple-particle reinforcement resulted in approximately equal tensile strength compared to MWCNT-GNP hybrid reinforcement. This can be due to the smaller content of each particle in triple-particle reinforcement (MWCNT-GNP-alumina) compared to double-particle (MWCNT-GNP) and single type reinforcement. For instance, if 20 g resin is selected for dispersion, single-type reinforcement with 0.1 wt% equals to 0.02 g of a specified particle, while, in double-type and triple-type reinforcement, the portion of each particle is 0.01 g and 0.0067 g, respectively. Hence, for 0.1 wt% content, smaller portion related to each particle in triple-particle reinforcement may not be enough to activate effective toughening mechanisms. For 0.3 wt% content, triple-particle reinforcement by MWCNT, GNP, and alumina using dispersion procedure B led to 3.6% and 9.0% improvements in tensile strength compared with double-particle reinforcement by MWCNT-GNP and single-particle reinforcement by GNP, respectively. For 0.5 wt%, using dispersion procedure

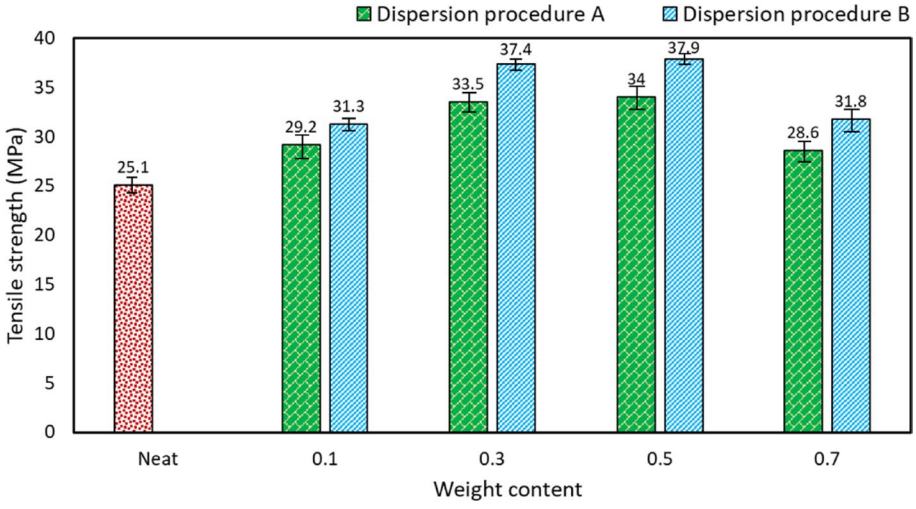


**Fig. 6** Average tensile strength of bulk adhesive specimens reinforced by triple insertion of MWCNT, GNP, and nano-alumina

B for triple-particle reinforcement revealed approximately equal tensile strength compared to double-particle reinforcement with GNP and MWCNT particles, while it had 19.2% higher tensile strength compared to maximum single-type reinforcement, which is related to alumina-reinforced adhesives. In can be inferred that, in the case of 0.5 wt%, although triple-particle reinforcement led to approximately equal tensile strength compared to double-particle reinforcement by MWCNT and GNP, it can be a cost-effective option due to the smaller weight portion of expensive particles of MWCNT and GNP. In addition to the aforementioned observations regarding Fig. 6 (triple-particle reinforcement), a comparison of the tensile strength of the triple-particle reinforced specimens prepared using dispersion procedure B with those of the double-particle reinforced specimens (Fig. 5) at each corresponding weight contents indicates that no substantial improvement is achieved through simultaneous incorporation of three nanoparticles (Table 3). Nevertheless, this approach can still be considered cost-effective, as it provides comparable strength enhancements while requiring smaller amounts of the costly nanoparticles (MWCNT and GNP).

In the single-particle reinforcement, for each specified weight content, the major reason of difference in tensile strength of various nanoparticles can be due to the difference in reinforcing mechanisms related to each particle. However, the idea of inserting a mixture of two or more particles in the hybrid reinforcement can lead to activation of different microstructural toughening mechanisms related to each particle as well as synergistic effects due to the particles [27, 39, 40, 49]. Schematic presentation of the microstructural phenomenon in the triple-particle reinforcement is illustrated in Fig. 7. As shown in the figure, as a crack is initiated in the polymeric matrix and approaches a MWCNT and GNP particle, due to the higher stress magnitudes in the vicinity of crack tip, MWCNT and GNP particles absorbs the energy and can be pulled-out from the matrix. Moreover, partial pull-out of GNP layers can occur in the case that the peel stresses on the GNP surface is not enough to overcome the adhesion force between the GNP layer and polymeric matrix. Also, breakage and deformation of GNPs can be introduced as other toughening mechanisms [36]. Due to pull-out of nano-sized spherical-shaped nano-alumina particles, plastic void growth can occur which can cause a local plastic effect in the polymeric matrix [40]. Moreover, deviation in crack growth path can be introduced as another energy absorbing mechanism which can occur due to the presence of all particles. Also, it should be noted that different morphologies of particles which are in tubular, planar, and spherical shapes can increase the possibility of deviation in crack growth path mechanism as the crack can propagate in different planes. As presented in Fig. 7, scanning electron microscopy (SEM) images show the evidences of pull-out of MWCNT, partial pull-out of GNPs, and plastic void growth due to pull-out of nano-alumina in the triple-particle reinforced adhesive specimen group. As previously discussed for Figs. 4 and 5, the schematic representations and microscopic images presented in Fig. 7 further serve as evidence of the dominant reinforcing mechanisms induced by the presence of each nanofiller within the epoxy adhesive matrix. Moreover, it can be inferred that the synergistic interaction among these mechanisms—resulting from the simultaneous incorporation of two or more types of nanofillers into the adhesive layer and the consequent enhancement of a specific mechanical property—is directly associated with the combined toughening mechanisms contributed by each individual nanoparticle. Thus, synergistic effects of the mechanisms activated

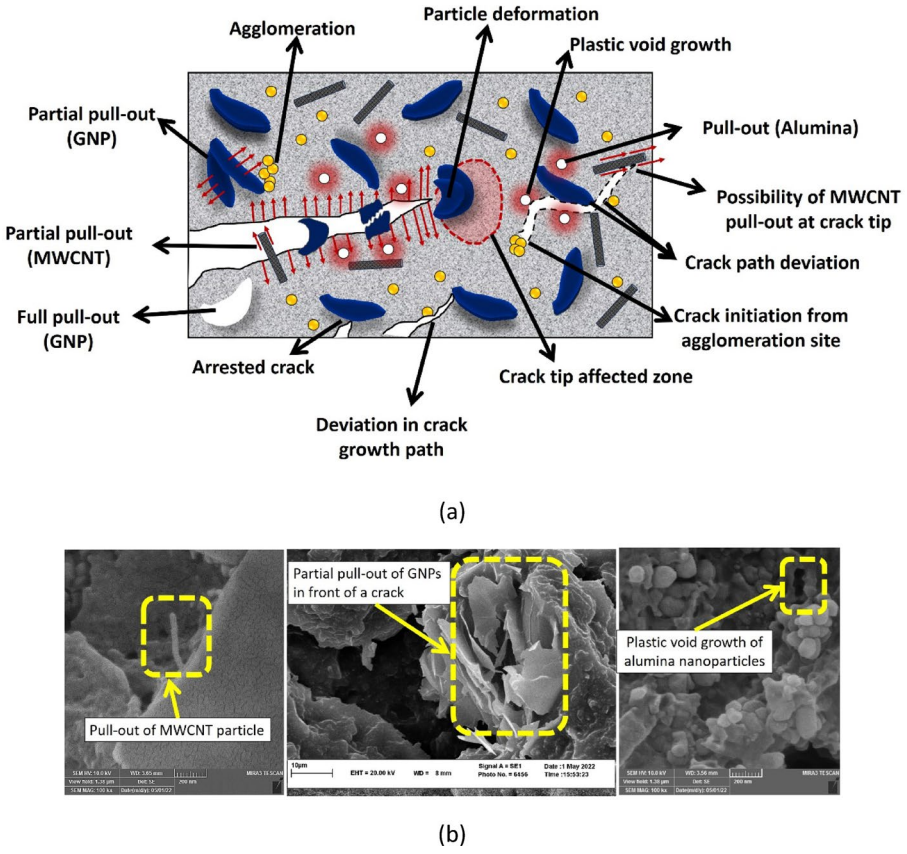


**Fig. 7** Microstructural mechanisms, (**a**) schematic presentation, (**b**) scanning electron microscopy images

by different particles can be known as the major microstructural reason of considerable tensile strength improvement in triple-particle reinforcement. Another key point to highlight is that the incorporation of nanoparticles with different morphologies and size scales can activate toughening mechanisms operating at various micro-mechanical levels. The authors refer to this phenomenon as multi-scale toughening mechanism activation. For example, semi-spherical nano-alumina particles are capable of arresting or deviating cracks within tens to hundreds of nanometers, whereas the planer morphology of GNPs-with diameters ranging from 1 to 20 μm-can arrest crack propagation at the micrometer scale of the crack length and crack tip opening displacement. Therefore, the hybrid incorporation of nanoparticles with distinct morphologies and dimensional scales can synergistically promote multi-scale toughening mechanism activation.

## 5 Conclusions

This study explored a novel approach to enhancing the tensile strength of an epoxy adhesive through single-, double-, and triple-particle nanoparticle reinforcement strategies using multi-walled carbon nanotubes (MWCNTs), graphene nanoplatelets (GNPs), and nano-alumina. The results highlighted that while each nanoparticle individually contributed to strengthening the adhesive matrix—particularly GNPs at 0.5 wt% yielding a 36.7% improvement—the hybrid reinforcement offered superior benefits when optimized. Among the hybrid configurations, the double-particle reinforcement type combining MWCNT and GNP at 0.5 wt% exhibited the highest tensile strength, with a 48.2%

increase over the neat adhesive and a 8.5% enhancement over the best single-particle result (GNP-reinforced adhesive with 0.3 wt% content).

The results indicated that reinforcing the adhesive with three nanoparticles, using the same dispersion procedure as that employed for the single- and double-nanoparticle specimen groups, was not able to compete with the highest performance achieved in the double-nanoparticle reinforced group (MWCNT–GNP at 0.5 wt%). However, when a modified particle-addition sequence was applied—namely, performing magnetic stirring and ultrasonic bath treatment after the addition of each nanoparticle—the tensile strength improved by approximately 2% relative to the maximum strength obtained in the dual-nanoparticle group. At 0.3 wt%, this modified dispersion approach led to a 3.6% and 9.0% enhancement compared to the double-particle (MWCNT-GNP) and the best single-type (GNP) systems, respectively. These findings suggest that although the triple-particle reinforcement provided a noticeable improvement compared with the dual-nanoparticle samples, at a specified weight content and under an equal mixing ratio condition, a smaller amount of each nanoparticle is used compared with the dual-nanoparticle formulation. This makes the triple-particle reinforcement approach more cost-effective for adhesive-performance enhancement processes.

Microscopic observations revealed that combining three nanoparticles—platelet-shaped GNP, tubular MWCNT, and spherical alumina—with distinct characteristic length scales activates reinforcing mechanisms (Pull-out, particle breakage, and crack path deviation for GNP, pull-out for MWCNT, and plastic void growth for alumina) across different microstructural levels and at various stages of damage initiation within the epoxy matrix. This synergistic activation enhances the reliability of micro-damage suppression and contributes to the overall improvement in mechanical performance.

## 6 Challenges and perspective to future researches

These findings highlight the potential of triple-particle reinforcement as a novel approach in adhesive engineering, underscoring the crucial role of dispersion techniques in achieving synergistic effects in multi-nanoparticle systems. This work lays the groundwork for more advanced hybrid adhesive formulations with superior mechanical performance. Accordingly, results of the present research study reveal some challenges in the context of hybrid nanoparticle reinforcement of adhesives, particularly in systems involving more than two nanoparticles (e.g., triple-particle reinforcement):

- Dispersion procedures used for single- or double-particle reinforcement may not be effective for systems with more complex hybrid reinforcements. Therefore, modifying the parameters or methods to achieve uniform particle dispersion poses a significant challenge.
- Depending on the types of nanoparticles used, selecting or adjusting the dispersion procedure is a critical step. A method suitable for one type of nanoparticle may cause damage to another, highlighting the need for tailored approaches.
- To optimize cost-effectiveness and enhance mechanical properties at a given weight content, using equal portions of each nanoparticle is not necessarily the best option. Therefore, targeted research is still required to investigate how different mixing ratios influence toughening mechanisms and property enhancement.
- Double- and triple-particle reinforcement strategies can be advantageous for simultaneously enhancing multiple adhesive properties, such as thermal and

mechanical performance. Thus, selecting nanoparticle combinations based on targeted multi-property improvements offers a promising roadmap for future research.

**Author contributions**
P. Zamani: Conceptualization, Methodology, Investigation, Data Curation, Writing - Original Draft, Supervision. Esmaeil Ghasemi solokloo: Investigation, Writing - Original Draft, Data Curation, Visualization. Ozkan Ozbek: Methodology, Validation, Writing - Original Draft. Mehmet Veysel Cakir: Methodology, Validation, Writing - Original Draft.Mahmoud Shariati: Conceptualization, Methodology, Validation, Supervision. Ali Hoseinzadeh: Methodology, Investigation, Visualization.

**Funding**
This research did not receive any specific grant from funding agencies in the public, commercial, or not-for-profit sectors.

**Data availability**
The datasets used and/or analysed during the current study are available from the corresponding author on reasonable request.

## Declarations

**Ethics approval**
This study does not involve human participants, animal subjects, human or animal data, or biological materials. Therefore, ethical approval was not required.

**Non-financial interests**
The author *Pedram Zamani* is an Editorial Board Member of Discover Mechanical Engineering and a Guest Editor of the Topical Collection associated with this submission. To avoid any potential conflict of interest, he had no involvement in the editorial handling, peer review, or final decision regarding this manuscript.

**Consent to publish**
Not applicable.

**Consent to participate**
Not applicable.

**Dual publication statement**
The results, data, and figures presented in this manuscript have not been previously published and are not under consideration for publication elsewhere..

**Competing interests**
The authors declare no competing interests.

Received: 28 July 2025 / Accepted: 28 January 2026
Published online: 17 February 2026

**References**

1. Golaz B, Michaud V, Lavanchy S, et al. Design and durability of titanium adhesive joints for marine applications. Int J Adhes Adhes. 2013;45:150–7.
2. Bartczak B, Mucha J, Trzepieciński T. Stress distribution in adhesively-bonded joints and the loading capacity of hybrid joints of car body steels for the automotive industry. Int J Adhes Adhes. 2013;45:42–52.
3. Kupski J, Teixeira de Freitas S. Design of adhesively bonded lap joints with laminated CFRP adherends: Review, challenges and new opportunities for aerospace structures. Compos Struct. 2021;268:113923.
4. Babaee Kashani H, Shariati M, Tahani M, et al. Experimental and numerical investigation on failure of PVC foam core tapered sandwich composites under four-point bending. Eng Fail Anal. 2025;173:109450.
5. Masoudi Nejad R, Ghahremani Moghadam D, Hadi M, et al. An investigation on static and fatigue life evaluation of grooved adhesively bonded T-joints. Structures. 2022;35:340–9.
6. Zamani P, Jaamialahmadi A, da Silva LFM, et al. An investigation on fatigue life evaluation and crack initiation of Al-GFRP bonded lap joints under four-point bending. Compos Struct. 2019;229:111433.
7. Sousa FC, Zamani P, Akhavan-Safar A, et al. A comprehensive review of the S-N fatigue behaviour of adhesive joints. J Adv Join Processes. 2024;9:100178.
8. Hosseinzadeh A, Shariati M, Zamani P, et al. On residual mechanical behavior of aluminum-to-composite bonded joints after low velocity transverse impact. Int J Adhes Adhes. 2025;140:104025.
9. Javanmard Sistani A, Shariati M, Zamani P et al. Mode-I and II fracture behavior of metal-to-composite bonded interfaces with a graphene nanoplatelet-reinforced structural epoxy adhesive. In: Proceedings of the Institution of mechanical engineers, part L: journal of materials: design and applications. 2024. https://doi.org/10.1177/14644207241226609
10. Ayatollahi MR, Samari M, Razavi SMJ, et al. Fatigue performance of adhesively bonded single lap joints with non-flat sinusoid interfaces. Fatigue Fract Eng Mater Struct. 2017;40:1355–63.
11. Shahani AR, Pourhosseini SM. The effect of adherent thickness on fatigue life of adhesively bonded joints. Fatigue Fract Eng Mater Struct. 2019;42:561–71.
12. Kim JH, Park BJ, Han YW. Evaluation of fatigue characteristics for adhesively-bonded composite stepped lap joint. Compos Struct. 2004;66:69–75.

13. Wu G, Li D, Lai WJ, et al. Experimental and numerical evaluations on the effects of adhesive fillet, overlap length and unbonded area in adhesive-bonded joints. Fatigue Fract Eng Mater Struct. 2020;43:2298–311.
14. Zhang D, Huang Y. The bonding performances of carbon nanotube (CNT)-reinforced epoxy adhesively bonded joints on steel substrates. Prog Org Coat. 2021;159:106407.
15. Korkmaz Y, Gültekin K. Effect of UV irradiation on epoxy adhesives and adhesively bonded joints reinforced with BN and B4C nanoparticles. Polym Degrad Stab; 202. 2022. https://doi.org/10.1016/j.polymdegradstab.2022.110004
16. Konstantakopoulou M, Kotsikos G. Effect of MWCNT filled epoxy adhesives on the quality of adhesively bonded joints. Plast Rubber Compos. 2016;45:166–72.
17. Khabaz-Aghdam A, Behjat B, Marques EAS, et al. Effect of reduced graphene oxide on mechanical behavior of an epoxy adhesive in glassy and rubbery States. J Compos Mater. 2021;55:3839–48.
18. Sekiguchi Y, Houjou K, Shimamoto K, et al. Two-parameter analysis of fatigue crack growth behavior in structural acrylic adhesive joints. Fatigue Fract Eng Mater Struct. 2023;46:909–23.
19. Khoramishad H, Ebrahimijamal M, Fasihi M. The effect of graphene oxide nano-platelets on fracture behavior of adhesively bonded joints. Fatigue Fract Eng Mater Struct. 2017;40:1905–16.
20. Dai Y, Zan Z, Zhao S, et al. Mode II cohesive zone law of porous sintered silver joints with nickel coated multiwall carbon nanotube additive under ENF test. Theoret Appl Fract Mech. 2022;121:103498.
21. Nazari R, Hakimi R, Daneshfar M, et al. Improving mode I fracture response of glass fiber-epoxy composite adhesive joints using sanding treatment and MWCNTs inclusion. Discover Appl Sci. 2024;6:479.
22. Khoramishad H, Ashofteh RS, Pourang H, et al. Experimental investigation of the influence of temperature on the reinforcing effect of graphene oxide nano-platelet on nanocomposite adhesively bonded joints. Theoret Appl Fract Mech. 2018;94:95–100.
23. Tutunchi A, Kamali R, Kianvash A. Steel-Epoxy composite joints bonded with Nano-$TiO_2$ reinforced structural acrylic adhesive. J Adhes. 2015;91:663–76.
24. Soltannia B, Taheri F. Influence of nano-reinforcement on the mechanical behavior of adhesively bonded single-lap joints subjected to static, quasi-static, and impact loading. J Adhes Sci Technol. 2015;29:424–42.
25. Khashaba UA, Najjar IMR. Adhesive layer analysis for scarf bonded joint in CFRE composites modified with MWCNTs under tensile and fatigue loads. Compos Struct. 2018;184:411–27.
26. Kubit A, Zielecki W, Drabczyk M. Influence of nanoalumina particles on the static and high-cycle fatigue properties of peel-loaded adhesive-bonded joints. Strength Mater. 2016;48:515–23.
27. NajiMehr H, Shariati M, Zamani P, et al. Investigating on the influence of multi-walled carbon nanotube and graphene nanoplatelet additives on residual strength of bonded joints subjected to partial fatigue loading. J Appl Polym Sci. 2022;139:52069.
28. Dizaji SA, Khabaz-Aghdam A, Kandemir AC. Fracture surface evaluation of adhesively bonded dissimilar joints reinforced with nanoclay. J Adhes Sci Technol. 2025;39:1757–77.
29. Demircan O, Kalaycı A. Investigation of mechanical properties of nano hexagonal Boron nitride integrated epoxy adhesives in bonded GFRP and CFRP composite joints. Int J Adhes Adhes. 2024;133:103759.
30. Akpinar S, Ozel A. Experimental and numerical determination of the thermal cycle performance of joints obtained with nanostructure-doped nanocomposite adhesives. Compos B Eng. 2019;174:106959.
31. Vattathurvalappil SH, Haq M. Thermomechanical characterization of Nano-Fe3O4 reinforced thermoplastic adhesives and single lap-joints. Compos B Eng. 2019;175:107162.
32. Bali G, Topkaya T. Effect of graphene nano-particle reinforcement on the fatigue behavior of adhesively bonded single lap joints. Int J Adhes Adhes. 2023;120:103279.
33. Akpinar S, Demir K, Gavgali E, et al. A study on the effects of nanostructure reinforcement on the failure load in adhesively bonded joints after the subjected to fully reversed fatigue load. J Adhes. 2022;98:1972–97.
34. Kubit A, Bucior M, Zielecki W. The impact of the multiwall carbon nanotubes on the fatigue properties of adhesive joints of 2024-T3 aluminium alloy subjected to Peel. Procedia structural integrity. Elsevier B.V.; 2016. pp. 334–41.
35. Sadigh MAS, Marami G. Enhancing fatigue life in adhesively bonded joints using reduced graphene oxide additive: experimental and numerical evaluation. Int J Adhes Adhes. 2018;84:283–90.
36. Zamani P, Jaamialahmadi A, da Silva LFM. The influence of GNP and nano-silica additives on fatigue life and crack initiation phase of Al-GFRP bonded lap joints subjected to four-point bending. Compos B Eng. 2021;207:108589.
37. Prasad V, Sekar K, Varghese S, et al. Enhancing mode I and mode II interlaminar fracture toughness of flax fibre reinforced epoxy composites with nano $TiO_2$. Compos Part Appl Sci Manuf. 2019;124:105505.
38. Razavi N, Ayatollahi MR, Nemati Giv A, et al. Single lap joints bonded with structural adhesives reinforced with a mixture of silica nanoparticles and multi walled carbon nanotubes. Int J Adhes Adhes. 2018;80:76–86.
39. Zamani P, Alaei MH, da Silva LFM, et al. On the static and fatigue life of nano-reinforced Al-GFRP bonded joints under different dispersion treatments. Fatigue Fract Eng Mater Struct. 2022;45:1088–110.
40. Zamani P, FM da Silva L, Masoudi Nejad R, et al. Experimental study on mixing ratio effect of hybrid graphene nanoplatelet/nano-silica reinforcement on the static and fatigue life of aluminum-to-GFRP bonded joints under four-point bending. Compos Struct. 2022;300:116108.
41. Cakir MV, Kinay D. MWCNT, nano-silica, and nano-clay additives effects on adhesion performance of dissimilar materials bonded joints. Polym Compos. 2021;42:5880–92.
42. Radshad H, Khoramishad H, Nazari R. The synergistic effect of hybridizing and aligning graphene oxide nanoplatelets and multi-walled carbon nanotubes on mode-I fracture behavior of nanocomposite adhesive joints. In: Proceedings of the Institution of mechanical engineers, Part L: journal of materials: design and applications 2022; 236:764–1776.
43. Rao Q, Huang H, Ouyang Z et al. Synergy effects of multi-walled carbon nanotube and graphene nanoplate filled epoxy adhesive on the shear properties of unidirectional composite bonded joints. Polym Test; 82. Epub ahead of print 1 February 2020. https://doi.org/10.1016/j.polymertesting.2019.106299
44. Safaei MM, Abedinzadeh R, Khandan A, et al. Synergistic effect of graphene nanosheets and copper oxide nanoparticles on mechanical and thermal properties of composites: experimental and simulation investigations. Mater Sci Eng B. 2023;289:116248.

45. Ejaz M, Azad MM, Shah A, ur R, et al. Synergistic effect of aluminum trihydrate and zirconium hydroxide nanoparticles on mechanical properties, flammability, and thermal degradation of polyester/jute fiber composite. Cellulose. 2022;29:1775–90.
46. Sha JJ, Lv ZZ, Lin GZ et al. Synergistic strengthening of aluminum matrix composites reinforced by SiC nanoparticles and carbon fibers. Mater Lett. 2020. https://doi.org/10.1016/j.matlet.2019.127024
47. Alies MSI, Khalil NZ. Effect of alumina/graphene hybrid nano reinforcement to the adhesion and mechanical properties of adhesively bonded aluminum alloy with epoxy. Mater Today Proc. 2022;51:1437–43.
48. Çakır MV. The synergistic effect of hybrid nano-silica and GNP additives on the flexural strength and toughening mechanisms of adhesively bonded joints. Int J Adhes Adhes. 2023;122:103333.
49. Özbek Ö, Çakır MV. MWCNT and nano-silica hybrids effect on mechanical and fracture characterization of single lap joints of GFRP plates. Int J Adhes Adhes. 2022;117:103159.
50. Ghanbari Y, Fatolahi AR, Khoramishad H. Enhancing fracture performance of non-conductive composite adhesively bonded joints with magnetically aligned MWCNT/$Fe_3O_4$ hybrid nanofillers. Fatigue Fract Eng Mater Struct. 2025;48:1667–80.

## Publisher's note